

Coherent bremsstrahlung produced by relativistic positrons and electrons on a single crystal of silicon*

R. L. Walker,[†] B. L. Berman, and S. D. Bloom

Lawrence Livermore Laboratory, University of California, Livermore, California 94550

(Received 16 September 1974)

The spectral dependence of the forward coherent bremsstrahlung produced by beams of 28-MeV positrons and electrons incident upon a 5- μm thick single crystal of silicon was measured with a NaI photon spectrometer. Effects of channeling and perhaps of the nonvalidity of the first Born approximation were observed for beam directions near the $\langle 111 \rangle$ axis of the crystal. A coherent peak near 0.5 MeV for both electrons and positrons was observed for a compound-interference direction, in agreement with first-order theoretical calculations.

I. INTRODUCTION

Channeling of relativistic positrons and coherently produced bremsstrahlung from both electrons and positrons in single crystals of silicon have been observed in transmission and scattering measurements for incident particle energies from 16 to 28 MeV, using beams from the Lawrence Livermore Laboratory linear accelerator. The axial and planar channeling and the accompanying bremsstrahlung from relativistic electrons and positrons impinging upon thin (5- to 53- μm) single silicon crystals were studied earlier.¹ The data reported in Ref. 1 demonstrated strong channeling behavior for positrons, although the channeling data for electrons reflected an angular dependence upon the incident beam alignment which could not be explained from experiments conducted at lower energies.² Additional experiments^{3,4} at comparable energies have shown the same type of channeling response for electrons; the entire subject of channeling has been reviewed recently by Gemmell.⁵ Also, it was found that either type of charged particle generates coherently produced bremsstrahlung when incident at a small angle from a major direction in a crystal. In this early work, however, only total intensities of the bremsstrahlung were observed. The measurements reported upon here were undertaken in an effort to study the shape of the coherent bremsstrahlung spectrum, and to examine its dependence upon the charge of the bombarding particles and the orientation of the crystal axis with respect to the incident beam direction.

The phenomenon of coherent bremsstrahlung results from the periodicity of the reciprocal lattice, which allows the occurrence only of those lattice recoil momenta which satisfy both the Bragg condition and momentum and energy conservation. Observation of this interference effect is enhanced in experiments where the detected bremsstrahlung

photons are restricted by suitable collimation to near the incident particle direction.⁶

In 1956, Uberall⁷ used the Born approximation and a simple cubic crystal lattice to analyze the interference effect. He obtained an expression for the intensity change of the Bethe-Heitler cross section for bremsstrahlung resulting from interference effects which also took into account electron screening and lattice vibrations. Several experiments (for example, Refs. 8–10) verified the predicted enhancement and highlighted the structure resulting from the discrete nature of the reciprocal lattice. In 1963, Mozley and De Wire¹¹ pointed out that the observed coherent spectrum can be modified further by strong collimation of the emergent radiation, resulting in a line spectrum superimposed upon a reduced incoherent background.

Diambrini⁶ has reviewed both theory and experiments as of 1968. In general, the experiments have been conducted at GeV energies; to date, none have been conducted in the MeV region. Moreover, both the experimental and theoretical requirements, techniques, and results in the MeV region are so vastly different from those pertaining to the GeV region that little useful information can be obtained from a simple extrapolation. In the present paper, for example, the influence of positron and electron channeling on coherent bremsstrahlung production is examined, along with the dependence of the coherent bremsstrahlung spectrum upon incident particle angle and polarity.

II. THEORY

The conventional theoretical treatment of coherent bremsstrahlung in single crystals is based upon the first Born approximation.^{6,7,12,13} Computer programs based upon this approach have been used to compute the predicted photon spectra at high relativistic energies.^{14–16} The effects of

multiple scattering of the charged particles and of collimation of the photon beam are included in the calculations. However, for very small angles of incidence, the relative contribution of the second Born approximation can become comparable to the contribution from the first.¹⁷ This could introduce a sizable effect dependent upon the sign of the charge; the prediction is an increase in the coherent bremsstrahlung intensity for positrons and a decrease for electrons. Also, channeling of relativistic positrons and electrons^{1,3,4,18} has not been included in any theory to date. Axial channeling of positrons tends to keep the particles far from the strings of nuclei, thereby reducing the probability of the close encounters necessary for coherent bremsstrahlung production. Electron channeling, on the other hand, increases the probability for close-encounter interactions.

The validity of the Born approximation for the treatment of coherent bremsstrahlung has been discussed by several authors.^{7,12,17,19,20} In general, the Born approximation begins to fail for high atomic numbers, for photon energies near the high-frequency limit, and for low incident electron energies. Schiff¹⁹ pointed out that, even for small Z , the phase change of the wave function of an electron passing through a crystal can be very large. Hence, Bloch wave functions are more appropriate than plane wave functions when treating coherent bremsstrahlung. Ferretti,^{12,20} predicted that, for unitarity reasons at very high energy, the Born approximation had to break down completely. He later²¹ proposed a method for calculating coherent bremsstrahlung which is valid when the energy of the photon is very small compared to the incident particle energy, as is the case in the present experiment. Unfortunately, the treatment is valid for positrons only. Akhiezer *et al.*¹⁷ showed that at small angles of incidence the kinematical restrictions imposed by the allowed crystal recoil momenta lead to an increased relative contribution from the second Born approximation, and hence in the intensity ratio of positron- to electron-produced coherent bremsstrahlung.

The relative contribution of the second Born approximation becomes appreciable at low relativistic energies. For 28-MeV positrons and electrons incident at 1° from a major axis of a single crystal of silicon, the second Born approximation makes a relative contribution of about 12%.¹⁷ This effect will of course be intertwined with the effect of the channeling.

Although an exact treatment of the intensity of coherent bremsstrahlung is lacking, the qualitative features, such as the locations of the peaks, can be interpreted easily as the result of kinematical

limitations introduced by the reciprocal lattice. The energies of the peaks can be determined from the following approximate formula²²:

$$\frac{E}{E_0} \cong \frac{2E_0q_1 - q_2^2}{1 + 2E_0q_1}, \quad (1)$$

where E is the energy of the photon, E_0 is the total energy of the incident charged particle, q_1 is the longitudinal momentum transferred to the crystal, q_2 is the transverse momentum transferred to the crystal, and normalized units ($\hbar = c = m_0 = 1$) are used. Equation (1) is based upon the assumptions $E \ll E_0$ and $E_0 \gg 1$. The transverse momentum term in Eq. (1) represents the curvature of the "momentum pancake"^{6,7} so prominent at lower energies. Both q_1 and q_2 have allowed discrete values; it should be noted that q_1 and q_2 must satisfy the conditions,^{6,7}

$$E/2E_0^2 < q_1 \lesssim 2/E_0 \quad \text{and} \quad 0 < q_2 \lesssim 4. \quad (2)$$

Photon collimation (or second collimation)^{11,22} causes the coherent bremsstrahlung peaks to become narrower, approaching line spectra as the collimator angles are reduced. Also, it reduces the incoherent bremsstrahlung intensity (whose angular distribution is broader).

Thus, for positrons and electrons incident at small angles from major directions in single crystals we should expect competing trends in the theoretical predictions from the effects of channeling and of taking into account the second Born approximation. As the angle of incidence is decreased, the intensity of coherent bremsstrahlung will increase for positrons until channeling becomes significant. (Axial-channeling half angles for silicon single crystals are on the order of two mrad for incident particle beams with energies of some tens of MeV; it is reasonable to expect relatively thin crystals, 5 to 50 μm , to exhibit strong channeling response to particle beams having divergences of about one mrad.) Once the particle beam is incident within the angular range for channeling, a strong reduction for close-encounter interactions should result for positrons. Electron channeling, on the other hand, keeps the particle near the atomic string, thereby increasing the probability for close-encounter interactions. It is noted, however, that electrons channel in an oscillatory manner around one atomic string, and thus are very susceptible to becoming dechanneled by thermal and zero-point motion, whereas positrons channel for relatively long distances, and are almost unperturbed by lattice motion.

III. EXPERIMENT

The experimental procedures were similar to those of Ref. 1. The apparatus is shown in Fig. 1.

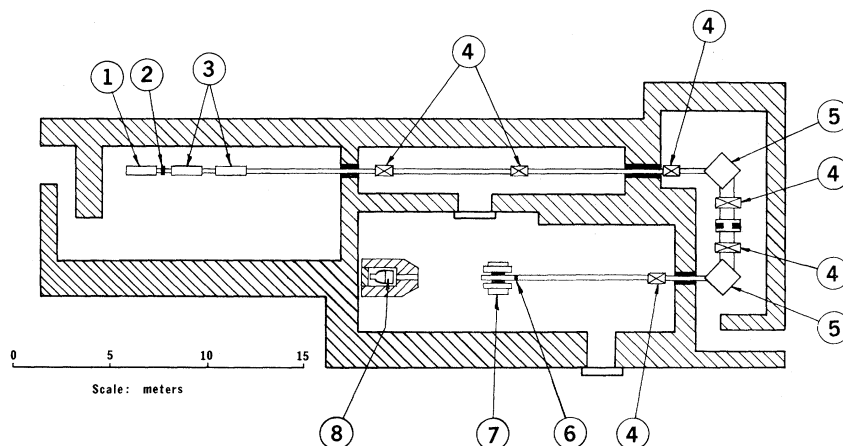


FIG. 1. Experimental apparatus. The high-current electron beam from the first accelerator section ① struck the 0.25-cm thick tungsten positron converter ②, producing in turn bremsstrahlung and positron-electron pairs in the converter, which were captured into the next accelerator section. By selecting the phase of the radiofrequency power to the subsequent accelerator sections ③ to be either the same as or opposite to that in the first section, either electrons or positrons were accelerated in the rest of the machine. The charged-particle beam was energy analyzed, transported to the experimental room, and focused into a nearly parallel beam by the bending and focusing magnets ④ and ⑤. The analyzed beam then impinged upon the thin silicon single-crystal bremsstrahlung target ⑥, and the transmitted beam was swept out of the 0° line of sight by the sweeping magnet ⑦. The collimated beam of forward bremsstrahlung photons was detected with the NaI(Tl) photon spectrometer ⑧.

Beams of 28-MeV positrons and electrons were obtained from the linear accelerator and energy analyzed with a bending-magnet-and-slit system to an energy spread of less than 1%. The beam was collimated in such a way that it was nearly parallel (see below) when it was allowed to strike a $5\text{-}\mu\text{m}$ -thick single crystal of silicon. The charged-particle beam, after having passed through the crystal, was bent down at a 50° angle by a sweeping magnet into a 3-m-long dumphole underground, at the end of which it was monitored by a plastic scintillator detector. The forward beam of bremsstrahlung photons produced in the silicon crystal was itself collimated (see below) and viewed with a 12.5-cm-diam-by-15-cm-thick NaI(Tl) photon spectrometer positioned 5 m downstream from the silicon crystal. The 1.25-cm-diam silicon crystal was cut so that the short dimension ($5\text{ }\mu\text{m}$) was nearly parallel to the (111) crystallographic direction, and was mounted on a goniometer capable of rotating the crystal through a two-dimensional angular range in 0.04-mrad steps.

The collimation system, which limits the momentum transferred by the incident charged particle to the crystal lattice, is shown in Fig. 2. The maximum (full-angle) beam divergence allowed was 4 mrad, corresponding to an optimum (full-angle) divergence of half this value. However, careful tuning of quadrupole magnets in the beam-transport system resulted in a beam quality which was considerably better than these geometrical

limits. This was borne out by the observation that positron-transmission measurements performed both with this set and with a much more restrictive set of collimators yielded essentially the same apparent channel widths. The upstream 1.6-cm-diam carbon collimator was selected to reduce the bremsstrahlung yield from that background source. Although the silicon-crystal target was 1.25 cm in diameter, the downstream 0.5-cm-diam lead collimator and the 45-cm-thick 0.95-cm-diam lead collimator positioned directly in front of the NaI detector allowed the latter to view only the central area of the silicon target.

The orientation of the single crystal mounted in the goniometer was determined by the channeling response of transmitted positrons. The single crystal initially was grown and prepared with the (111) direction nearly normal to its surface. It was mounted on the inner gimbal ring of the goniometer and adjusted until the crystal showed no optical distortion. A positron mapping was performed to locate the string position and the (110) planes. This was accomplished by measuring the transmitted positron beam with a plastic scintillator as a function of the goniometer settings, as was reported in Ref. 1, and observing the large increase in the transmitted positron intensity when the crystal was swept through a channeling direction. The data set generated by this procedure is shown in Fig. 3. This technique allowed the crystal to be oriented to within 0.1 mrad, an uncertainty much smaller than the probable beam

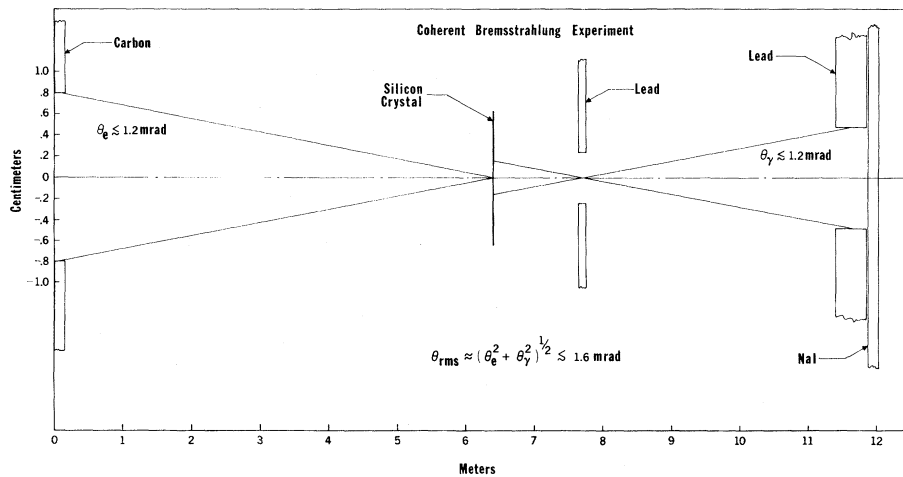


FIG. 2. Collimation system. The 15-cm-thick graphite collimator limited the charged-particle beam diameter at the position of the last quadrupole focusing magnet. The 10- and 46-cm thick lead collimators limited the part of the silicon crystal viewed by the photon spectrometer as well as the angular divergence of the forward bremsstrahlung beam.

divergence involved.

The electronics and data-recording equipment were straightforward. The amplified output signals from the NaI spectrometer were split and fed both to a 1024-channel pulse-height analyzer having a threshold for valid events (well above noise level) corresponding to 162-keV photons, and to a single-channel analyzer having a threshold of 12.5 MeV, for normalization purposes. Both analyzers were gated by a trigger pulse from the linear accelerator so that events occurring from cosmic rays and other machine-off background sources were reduced to a negligible rate. The counting rate of stored pulses was monitored and used to hold the beam intensity at a (low) con-

stant level, so that pile-up corrections were small (< 3%). A ^{22}Na γ -ray source was used to calibrate the energy scale. The accelerator was operated at 360 Hz (1- μ sec pulses); the experimental runs each were a few hours long, during which the counting rate never exceeded 10 sec^{-1} .

Eight kinds of data runs were taken, for both incident positrons and electrons and for each of four orientations of the target crystal: on-channel, on-shoulder, compound, and random (Figs. 4 and 5). In the on-channel position, the particle beam was collinear with the $\langle 111 \rangle$ string direction (within the limits of divergence of the beam). The on-shoulder spectrum was measured with the particle beam incident along a (110) plane, 15 min of arc from the string direction. In the compound posi-

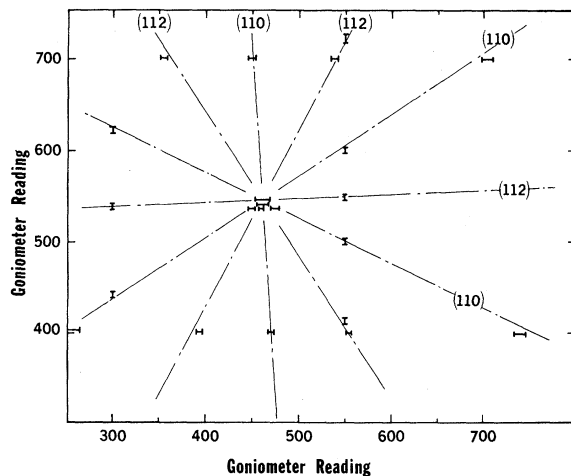


FIG. 3. Planar-channeling map of the 5- μ m-thick silicon crystal. Wide-angular-range scans of the transmitted positron beam were made, and the location of the various planar-channeling peaks form a data set which allows the mapping of the major planes which intersect the principal $\langle 111 \rangle$ crystallographic direction. This mapping technique was used to orient the crystal with a high degree of precision.

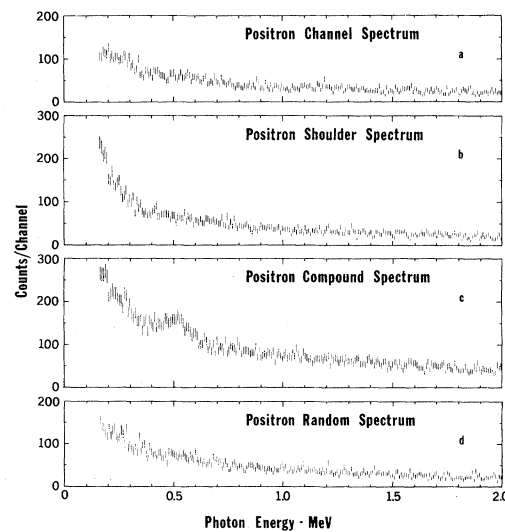


FIG. 4. Unnormalized photon spectra for incident positrons: (a) on-channel spectrum; (b) on-shoulder; (c) compound; (d) random. No backgrounds have been subtracted from the data (see text).

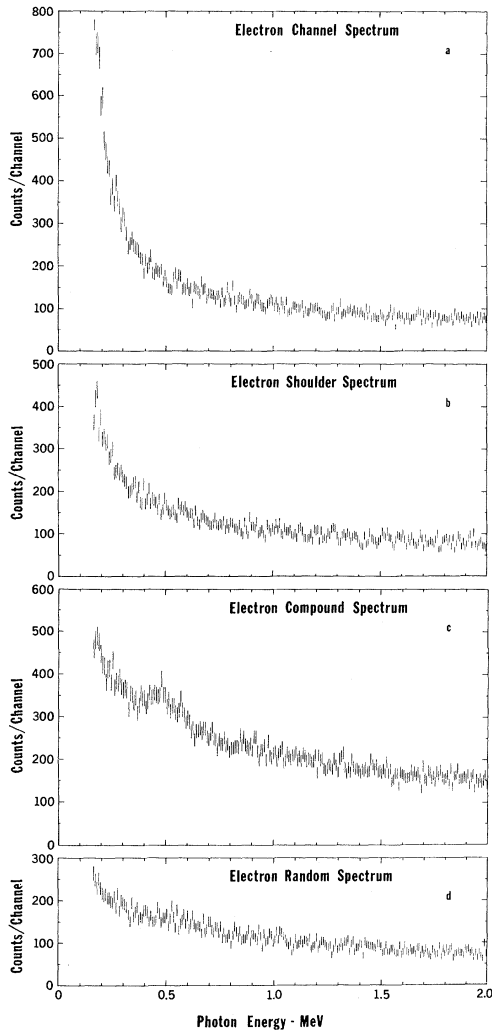


FIG. 5. Unnormalized photon spectra for incident electrons: (a) on-channel spectrum; (b) on-shoulder; (c) compound; (d) random. No backgrounds have been subtracted from the data (see text).

tion, the particle beam was incident along a (110) plane, 50.5 min of arc from the string direction. Finally, the random-position spectra were measured at an orientation selected far from the string direction and major planes. The electron beam intensity was about three times as great as the positron beam intensity. Four electron spectra were measured with a high-energy (≥ 12.5 -MeV) normalization of 1.5×10^4 counts and one compound spectrum was normalized to 3×10^4 counts. Four positron spectra were measured with a high-energy normalization of 0.5×10^4 counts and one compound spectrum was normalized to 1×10^4 counts.

Backgrounds were shown to be negligible by means of beam-off and target-out runs, the latter performed at other times but with the same experimental geometry. No backgrounds have been

subtracted from the data in the figures, but it should be noted that whatever (small) background is present (a) will be present in nearly proportionate amounts in all the spectra, and (b) will tend only to emphasize further the difference between the relative sizes of the coherent peak for positrons and electrons shown in Figs. 4(c) and 5(c).

IV. RESULTS AND DISCUSSION

The results are shown in Figs. 4–7. Figure 4 shows the unnormalized photon spectra for the four positron runs, and Fig. 5 shows those for the electron runs. The on-shoulder spectra [Figs. 4(b) and 5(b)] and the on-channel spectrum for electrons [Fig. 5(a)] show the enhancement of low-energy bremsstrahlung [relative to the random spectra shown in Figs. 4(d) and 5(d)] expected from the results of Ref. 1. Since the positrons, being positively charged, are repelled from the lattice sites (the atomic nuclei) when the beam is directed along the string direction, bremsstrahlung production in general is inhibited for this case, the coherence effect is suppressed, and hence the spectrum of Fig. 4(a) does not show any significant low-energy enhancement. Indeed, the present collimation assured that the maximum beam divergence still lay within the channeling half angle (which was in fact measured for this crystal in a subsidiary experiment); therefore, one can assume that the positrons were well channeled and only dechanneled positrons contributed to the bremsstrahlung production, resulting in a photon spectrum shape comparable to one for a random orientation of the crystal.

The low-energy bremsstrahlung enhancement can be seen more clearly in Fig. 6. Here are plotted the normalized differences between the spectra of Figs. 4(b) and 4(d) [Fig. 6(a)], Figs. 5(b) and 5(d) [Fig. 6(b)], and Figs. 5(a) and 5(d) [Fig. 6(c)]. These normalizations equated the number of counts above 12.5 MeV for the various pairs of runs, on the reasonable assumption that all coherent effects in the high-energy region of the bremsstrahlung spectra are negligible. The on-shoulder position was chosen to investigate the bremsstrahlung spectra for particles in the angular range where the “shoulders” of the channeling response are prominent.¹ The low-energy bremsstrahlung enhancement for on-shoulder incident positrons [Fig. 6(a)] exceeds that for the comparable electron data [Fig. 6(b)]. This could be explained by the need for taking into account the second Born approximation for this case. The influence of axial channeling is dramatized by the large low-energy enhancement for on-channel incident electrons [Fig. 6(c)]; presumably this results from the electrons being attracted to the

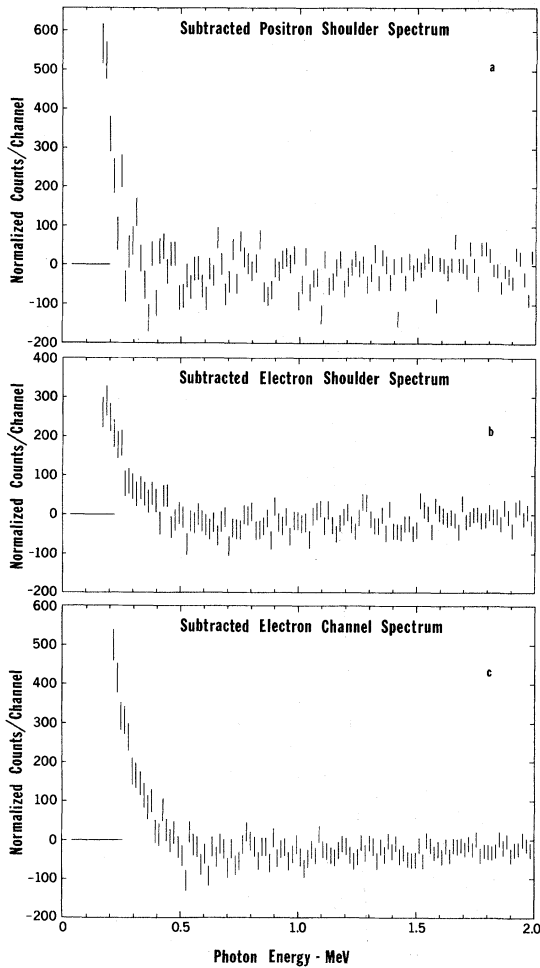


FIG. 6. Normalized difference spectra, showing the low-energy bremsstrahlung enhancement: (a) on-shoulder-minus-random spectrum for positrons; (b) on-shoulder-minus-random spectrum for electrons; (c) on-channel-minus random spectrum for electrons.

string of atomic nuclei, as contrasted with the case for positrons.

The photon spectra for the cases when the orientation of the silicon crystal, relative to the direction of the incident beam, was adjusted for compound interference are shown in Figs. 4(c) and 5(c). Both these spectra contain a striking peak near 0.5 MeV, although the peak is at least twice as prominent in the positron data [Fig. 4(c)]. The kinematics of the coherent bremsstrahlung process results in the prediction [from Eq. (1)] of a clustering of coherent strength near 0.5 MeV for the compound interference position chosen here for study, in agreement with the present experimental results. Although the charged-particle beam optics were not precisely the same for the two cases, it still is likely that channeling, with perhaps some contribution from the second-Born-

approximation effect, account for the relatively greater enhancement of the coherent peak in the positron data.

We also note that for the shoulder position a coherent bremsstrahlung peak should occur at 0.13-MeV and higher-order peaks approximately at integral multiples of this energy. However, the lowest-order shoulder peak is below the threshold set on the NaI detector, and the higher-order peaks are too weak to be discernible. Higher-order peaks also should occur in the compound-position spectra. Such peaks are predicted [Eq. (1)] to lie near 1.1 and 1.7 MeV, but should have intensities much smaller than that for the one near 0.5 MeV. Figure 7 shows the data up to 4 MeV for these spectra; it does not appear that these or any other higher-order peaks have been observed. Also, in both the shoulder and compound positions planar channeling might have some influence on the data, but no apparent effect is discernible [the (110) planar-channeling angles are approximately $\frac{1}{3}$ of the (111) axial-channeling value].

As a final note, it is worth commenting on the application of Eq. (1) to the peak at $E \approx 0.5$ MeV. There are, of course, a very large number of sets of (q_1, q_2) which contribute to this observed peak. Choosing a representative point in this set, we find the approximate results:

$$q_1 \approx 0.029 \quad \text{and} \quad q_2 \approx 1.78,$$

which satisfy conditions (2). Substituting these values into Eq. (1) results in the scaling law

$$\frac{E}{E_0} \cong (0.058E_0 - 3.17)/(1 + 0.058E_0), \quad (3)$$

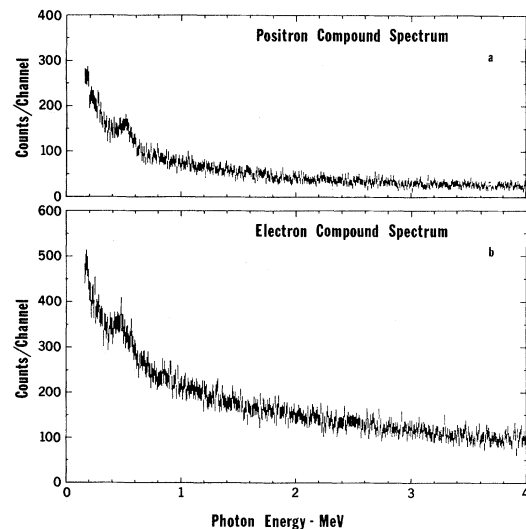


FIG. 7. Unnormalized photon spectra up to 4 MeV for the compound-interference case: (a) for incident positrons; (b) for incident electrons.

where all energies are expressed in units of m_0c^2 (0.511 MeV). It can be seen that a mere doubling of E_0 results in an increase of E/E_0 of considerably more than a factor of 10; now, however, E no longer is much smaller than E_0 , which means that a more rigorous relation than Eq. (3) is required to predict properly the scaling properties of the peaks of the coherent bremsstrahlung. Nonetheless, whatever a more reliable theory might predict, it is clear that the production of monochromatic coherent peaks in the MeV region is not an unreasonable objective, which, of course, was one of the main driving purposes of this experiment.

V. SUMMARY

When bremsstrahlung was established as an observable in channeling experiments,¹ it was noted that the response resulted primarily from low-energy photons. It now has been shown clearly that the low-energy component indeed owes its origin to coherent bremsstrahlung. The spectral shape of the low-energy component has been examined, and a specific peak of coherent brems-

strahlung for a compound-interference direction has been observed. The position of this peak is consistent with first-order theory within the experimental accuracy of the measurement.

It is clear that certainly channeling and perhaps the nonvalidity of the first Born approximation must be considered when studying coherent bremsstrahlung generated by relativistic positrons and electrons in the MeV region. The data gathered from this experiment highlight the significance of the former and suggest the investigation of the latter with more high-resolution experimental measurements.

ACKNOWLEDGMENTS

The authors would like to thank R. C. Der for help in taking the data; Dr. J. M. Khan, Dr. T. M. Kavanagh, Professor C. Kittel, and especially Dr. T. F. Godlove and Dr. A. W. Saenz for valuable discussions; T. C. Madden and the Bell Telephone Laboratories for providing us with the silicon crystal; and E. Dante, H. Fong, and the other accelerator operators for their wizardry in producing parallel positron and electron beams.

*Work performed under the auspices of the U. S. Atomic Energy Commission. Preliminary accounts of this work appeared in *Bull. Am. Phys. Soc.* **18**, 141 (1973), and *Proceedings of the International Conference on Photonuclear Reactions and Applications*, edited by B. L. Berman (Lawrence Livermore Laboratory, 1973), p. 247.

†Present address: Offutt Air Force Base, Neb. 68113.

¹R. L. Walker, B. L. Berman, R. C. Der, T. M. Kavanagh, and J. M. Khan, *Phys. Rev. Lett.* **25**, 5 (1970).

²E. Uggerhøj and F. Frandsen, *Phys. Rev. B* **2**, 582 (1970).

³H. Kumm, F. Bell, R. Sizmann, H. J. Kreiner, and D. Harder, *Rad. Effects* **12**, 53 (1972).

⁴A. Neufert, U. Schiebel, and G. Clausnitzer (private communication).

⁵D. S. Gemmell, *Rev. Mod. Phys.* **46**, 129 (1974).

⁶G. Diambri Palazzi, *Rev. Mod. Phys.* **40**, 611 (1968).

⁷H. Überall, *Phys. Rev.* **103**, 1055 (1956).

⁸G. Barbiellini, G. Bologna, G. Diambri, and G. P. Murtas, *Phys. Rev. Lett.* **9**, 396 (1962).

⁹T. Kifune, Y. Kimura, M. Kobayashi, K. Kondo, and T. Nishikawa, *J. Phys. Soc. Jpn.* **21**, 1905 (1966).

¹⁰G. Bologna, G. Lutz, H. D. Schulz, U. Timm, and W. Zimmermann, *Nuovo Cimento A* **42**, 844 (1966).

¹¹R. F. Mozley and J. De Wire, *Nuovo Cimento* **27**, 1281 (1963).

¹²B. Ferretti, *Nuovo Cimento* **7**, 118 (1950).

¹³M. L. Ter-Mikaelian, *Zh. Eksp. Teor. Fiz.* **25**, 296 (1953).

¹⁴R. F. Schwitters (private communication).

¹⁵T. Tsuru, S. Kurokawa, T. Nishikawa, S. Suzuki, T. Katayama, M. Kobayashi, and K. Kondo, *Phys. Rev. Lett.* **27**, 609 (1971).

¹⁶W. Saenz (private communication).

¹⁷A. I. Akhiezer, P. I. Fomin, and N. F. Shul'ga, *Zh. Eksp. Teor. Fiz. Pis'ma Red.* **13**, 713 (1971) [*Sov. Phys.—JETP Lett.* **13**, 506 (1971)].

¹⁸V. L. Morokhovskii, G. D. Kovalenko, I. A. Grishaev, A. N. Fisun, V. I. Kasilov, B. I. Shramenko, and A. N. Krinitsyn, *Zh. Eksp. Teor. Fiz. Pis'ma Red.* **16**, 162 (1972) [*Sov. Phys.—JETP Lett.* **16**, 112 (1972)].

¹⁹L. I. Schiff, *Phys. Rev.* **117**, 1394 (1960).

²⁰B. Ferretti and G. Gamberini, *Nuovo Cimento Lett.* **3**, 113 (1970).

²¹B. Ferretti, *Nuovo Cimento B* **7**, 225 (1972).

²²U. Timm, DESY Report No. 69/14 (1969) (unpublished).